

Article

Research on and Design of an Electric Drive Automatic Control System for Mine Belt Conveyors

Li Wang ¹, Haoxin Li ², Jingkai Huang ² , Jinbin Zeng ², Luxin Tang ³, Weibin Wu ² and Yuanqiang Luo ^{2,*}

¹ Guangzhou Institute of Science and Technology, College of Intelligent Manufacturing and Electrical Engineering, Guangzhou 510540, China

² College of Engineering, South China Agricultural University, Guangzhou 510642, China

³ Guangdong Industrial Robot Integration and Application Engineering Technology Research Center, Guangzhou Institute of Science and Technology, Guangzhou 510540, China

* Correspondence: luoyq@scau.edu.cn

Abstract: Conveyor belts are widely used in ore transportation in large-scale mines for their long transportation range, high safety, and strong economic applicability. Coal mine belt conveyors are not only traditional, simple mechanical conveying devices but also automatic control system operating devices that integrate safety, stability, and low power consumption. In the process of coal mining, a conveyor belt control system also needs to be closely integrated with modern industrial systems and information systems, which greatly improves its work efficiency. The purpose of this article is to improve the methods for designing automatic control systems for electric motors in order to obtain mechanical characteristics close to a constant power line, which would ensure the reliable operation of belt conveyors. An automatic control system was designed based on the controller Siemens S7-1200; then, a mathematical model of an automated electric drive was developed. Based on the mathematical model, a simulation model of an automatic electric drive was built, and the modes were modeled. After designing, the obtained plots of transients completely corresponded to the required transients, which means that the Siemens frequency converter automatic control system (ACS) parameters were calculated quite accurately and the conveyor electric drive met all requirements.

Keywords: conveyor belt; electric drive; automatic control systems; transmission technology



Citation: Wang, L.; Li, H.; Huang, J.; Zeng, J.; Tang, L.; Wu, W.; Luo, Y.

Research on and Design of an Electric Drive Automatic Control System for Mine Belt Conveyors. *Processes* **2023**, *11*, 1762. <https://doi.org/10.3390/pr11061762>

Academic Editor: Jean-Pierre Corriou

Received: 26 April 2023

Revised: 4 June 2023

Accepted: 6 June 2023

Published: 9 June 2023



Copyright: © 2023 by the authors. Licensee MDPI, Basel, Switzerland. This article is an open access article distributed under the terms and conditions of the Creative Commons Attribution (CC BY) license (<https://creativecommons.org/licenses/by/4.0/>).

1. Introduction

Belt conveyors are the most common type of conveying machines; they are used to move bulk goods. The core element of a mining conveyor is the conveyor belt. It is driven by drive–tension drums [1]. Mine belt conveyors are equipped with grooved roller bearings that ensure the stiffness and integrity of the construction and minimize the sagging of the belt. They minimize the risk of sagging under the weight of the load.

Mine belt conveyors are mainly used in tunneling work and mining applications, including coal mining. They are also used in underground construction and excavation work. This type of equipment is indispensable in sites where the working length needs to be changed periodically, for example, as the mine is excavated [2]. Belt mine conveyors are used in mines to deliver minerals and transport them through built-up drifts, cross ditches, sectional and capital ditches, and inclined shafts and drifts [3]. At present, scrapers and belt conveyors are widely used.

In a belt conveyor, rocks are transported on a conveyor belt that performs the function of a traction and bearing body. A closed, endless tape goes around the head drive and tail tension drums [4]. The belt is supported along the length of the conveyor by stationary roller supports, and the distance between the roller supports and the upper load branch is 2–2.5 times shorter than that between the roller supports and the lower empty branch [5]. Loading is possible at almost any point along the length of the conveyor. Typically, belt conveyors are loaded in the tail section using a hopper and are unloaded when the belt

leaves the head drum [6]. It is possible to unload the belt conveyor at intermediate points using plow ejectors or unloading carts. Depending on the purpose and operating conditions, belt conveyors are equipped with additional devices for cleaning the belt and drums and for catching the belt in case it breaks [7]. To control the operation and automation of conveyors, various sensors and devices are installed [8].

The advantages of belt conveyors are high productivity, long length of both one line and the entire conveyor line, relative simplicity of design, significantly lower weight and specific energy consumption than scraper conveyors, high reliability, safety and the possibility of the full automation of work, while their disadvantages are limitations in the size of the transported rock mass (up to 500 m), the need for straight-line installation of the conveyor planned, a limited angle of inclination, high cost, and relatively short service life [9]. In ore mines, depending on the operating conditions, belt conveyors with belt widths of 650, 800, 1000, 1200, and, less often, 1600 and 2000 mm are used [10].

In the domestic industry, for the underground transport of coal and in ore mines, conveyor belts are produced according to the standard range, the main parameter of which is the width of the belt. The following are models of belt conveyors: L—belt; LB—bremsberg ribbon; LT—telescopically shortened tape; LTP—telescopic tape (extensible tunneling); LN—tape for inclined working surfaces with inclination angles of up to $\pm 25^\circ$ [11]. In the designation of the conveyor type, the numbers to the right of the main letter index correspond to the width of the belt in centimeters; the numbers to the left correspond to the standard size of the drive station; and the letter index to the right of the number corresponds to the conveyor version [12–14]. In the designation of conveyors assembled from unified blocks, the letter U is added to the right. In the extraction from manganese ores with long pillars with recesses (Nikopol deposit), sectional belt conveyors of the KLZS2 type are used for down-hole transport. In addition, belt conveyors of the KLZ-500 and KL-600 types are used to transport potash ores on panel working surfaces. For the transportation of potash ore along capital horizontal and inclined working surfaces, belt conveyors of a unified series of types 1L120 and 2L120 are used. In the extraction from ores of ferrous and non-ferrous metals and in the mining of chemical raw materials, for the transportation of crushed ore with a particle size of 200–250 mm along inclined shafts, 2L120A and 2L120BM belt conveyors are used. The 2L120A belt conveyor includes a two-drum drive station, an external unloading drum, a tension station, a rigid frame, and a loading device. With a belt width of 1200 mm and a speed of 3.15 m/s, the technical performance of the conveyor is 1500 t/h, with total drive power of 1000 kW. The main difference between the 2L120B and 2L120A conveyors is as follows: an additional 500 kW electric drive is installed on the head remote drum (total power of 3×500 kW), and a stronger tape, 2RTLO3150, is used.

The use of modern automated electric drives is of great importance for conveyor control. Therefore, the development of an automated electric drive for the main belt conveyor for moving ore is a hot topic.

2. Industrial Plant Description

A conveyor works as part of the panel conveying line. In the process of operation, the conveyor receives the materials conveyed by the previous belt conveyor (or scraper drift conveyor), conveys them along the panel, and transfers the materials to the next belt panel conveyor or trunk belt conveyor.

The 11200 belt conveyor is used for conveying potash ore or other rock mass (coal and shale) with grain size less than 300 mm along straight mines.

The main belt conveyor model MKL1-1200, with maximum length $L = 550$ m, was designed by Soligorsk Institute of Resource Efficiency Problems with Experimental Production [15–19].

The technical characteristics of the MKL1-1200 conveyor for basic installation are presented in Table 1.

Table 1. Technical Specifications of 11200 Conveyor.

| Technical Specification | Value |
|--|-------|
| Rated running speed of conveyor belt, m/s | 3, 10 |
| Tape width, mm | 1200 |
| Yield, t/h | 1200 |
| Length, m | 550 |
| Motor power, kW | 160 |
| Motor shaft speed and synchronization, revolution/minute | 1000 |
| Voltage, V | 660 |
| Transmission ratio of reducer | 20 |
| Drive drum diameter, m | 1, 2 |

2.1. Selection of Electric Drive Control Coordinates

The technological process of conveyors is very simple and can be summarized as conveying ore to conveyor drifts with panel conveyors equipped with an LI-1200 trunk belt conveyor (conveyor belt under consideration) “up the hill” along the trunk [20].

A transport drift is arranged in a direction parallel to the main conveyor drift, and a transformer is arranged in the drift. There is also a ventilated drift, which has a ventilated lintel and a mesh door between it and other drifts [21,22]. Electrical control equipment is installed after the ventilation jumper, including regulating equipment, a mine machine starter, a mine machine cabinet, a refrigeration unit, a BISUK1 control complex, and a belt conveyor. For the execution of power electrical equipment and lighting, mine explosion-proof (EP) equipment is used [23].

The main parts of the structure of the 11200 belt conveyor include an external head, a frame, a flexible belt, a fixed roller-bracket-supporting belt along the length of the conveyor, a belt-tensioning device, a drive station, and grounding wire [24].

The conveyor belt is the traction and bearing part of the conveyor belt and is composed of a strong skeleton and a protective rubber pad. Conveyor belts have the requirements of high longitudinal strength and transverse bending elasticity, low dead weight elasticity and residual elongation under longitudinal force, low hygroscopicity, and other requirements [25].

On a belt conveyor, the developed traction force is determined by the drive station with a unidirectional arrangement of drive units. The drive station of the MKL1-1200 conveyor consists of a motor, a reducer, and a brake. The drive unit of the MKL1-1200 conveyor consists of an electric motor and a reducer connected to the electric motor with a clutch [26]. TKTG-500 has a KMT-411A solenoid. On the gearbox, the output shaft is mounted, and a half coupling connects the gearbox and the intermediate shaft. The MKL1-1200 conveyor drive unit is equipped with an explosion-proof (EP) asynchronous electric motor, which is mounted on the gearbox’s side. The electric motor and gearbox are mounted on the frame. The frame is mounted on foundations using foundation blocks. The gearbox TSDN-710-20-U3 has two spur gear stages with a gear ratio of 20. The gears are enclosed in cast-iron housing.

The moving speed of the belt is selected based on the characteristics of the above-mentioned coordinate control electric drive process.

2.2. Formulation of Requirements

The requirement of a conveyor electromechanical drive is to obtain its four basic modes (starting, meeting production requirements, speed adjustment, and braking) and a series of auxiliary and debugging modes, and to ensure the reliable and smooth operation of the conveyor, as shown in Figure 1.

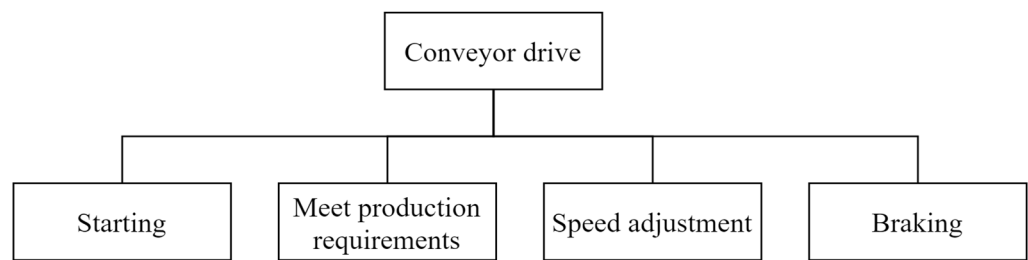


Figure 1. The requirements of a conveyor electromechanical drive.

The main requirements for the conveyor drive are as follows: It needs to ensure that the motor starts smoothly and has limited torque and acceleration values (the belt starting acceleration should not exceed 0.2 m/s^2) to ensure the shock-free selection of gear clearance during the initial period. The driving device is designed to limit the power of the traction device. The electric drive device should be able to meet the required output of 1200 tons/h. The electric drive device has weather resistance, configuration level 4, and protection level IP54. It needs to provide greater torque during startup, as the static friction resistance is approximately 1.5–2 times that of the moving friction resistance and there may be dirt in the mechanical walking part, causing the lubricating oil to solidify. According to the load of the conveyor belt, the frequency and value of the motor power supply voltage need to be changed to achieve speed regulation. To reduce the wear of the mechanical brake lining, one needs an electric brake. Starting from maximum speed, the mechanical brake should be activated.

3. The Automated Electric Drive

3.1. Functional Diagram of an Automated Electric Drive

The transmission device of the belt conveyor is used to transmit traction to the belt, set the required speed of the belt, and provide starting and stopping modes. The drive of a belt conveyor consists of a motor, a reducer, a clutch, and a brake. The transmission device of a conveyor can adopt a hydraulic or electromagnetic clutch. The determination of the transmission components of a belt conveyor and the selection of its control system should be based on the following knowledge: the operation mode of the conveyor; the number of driving rollers and motors; the position of the drive drum; the working conditions.

There are the following principles for varying the speed of a conveyor drive:

- Frequency control;
- Phase rotor adjustment;
- Hydraulic clutch speed regulation.

The introduction of variable frequency drives (VFDs) makes it possible to increase the reliability of equipment and systems, improve the quality of products and services produced, automate production, and save resources and energy.

However, frequency regulation also has a number of disadvantages: most VFD models are a source of interference; relatively high cost of high-power VFDs; the aging of the main circuit capacitors.

Frequency control has been effectively applied in energy, industry, and public utilities.

Squirrel-cage motors are the most common motors and have only recently been used for non-adjustable electric drives, because the almost only effective method for speed regulation, consisting in changing the frequency of the voltage applied to the stator windings, is technically difficult. Now, thanks to the success of electronic equipment, the situation has changed dramatically, and variable frequency electric drives have become the main type of adjustable electric drives. In Figure 2, U_{1H} and f_{1H} are the voltage and frequency of the power supply; U_1 and f_1 are the voltage and frequency output by the frequency converter; FC is the frequency converter; and ω is the angular velocity.

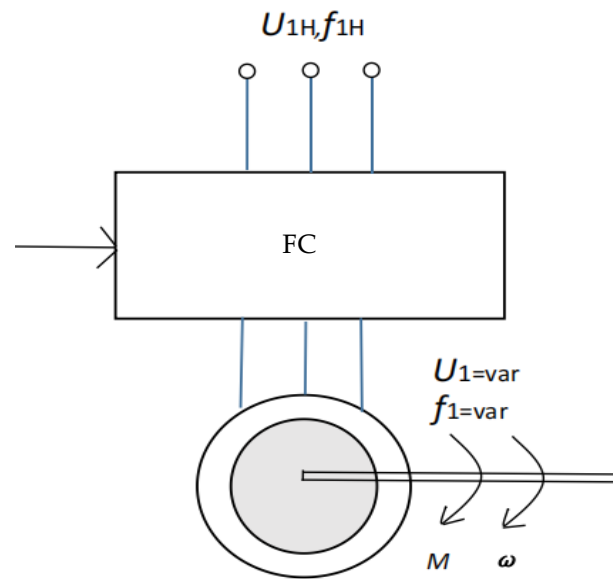


Figure 2. Schematic diagram of frequency conversion electric drive system.

In general, for machines with P antipoles ($P = 1, 2, 3 \dots$), the synchronous angular velocity is ω_0 , rad/s, defined as

$$\omega_0 = \frac{2\pi f_1}{p} \quad (1)$$

where f_1 is the frequency, Hz.

It can be roughly considered that the magnetic flux is determined by the applied voltage, frequency, and winding parameters.

$$\varphi = \frac{U_1}{4.44 f_1 \omega_1 k_{ob}} = \frac{U_1}{f_1} \quad (2)$$

As shown in Equation (1), ω_0 is proportional to frequency f_1 and does not depend on other values of the machine. When modifying f_1 , attention should be paid to the voltage amplitude, as when f_1 decreases, in order to maintain the magnetic flux at a certain level, for example, nominal level, $E_1 \approx U_1$ should be changed. Thus,

$$\frac{U_1}{f_1} = \frac{U_{1H}}{f_{1H}} = const \quad (3)$$

When the frequency increases from the rated frequency, $U_1 = U_{1i}$. The flow according to Equation (2) then decreases.

Let us evaluate frequency–speed regulation:

1. Regulation is dual-zone downregulation ($U_1/f_1 \approx const$) and upregulation ($U_1 = U_{1H}$, $f_1 > f_{1H}$) with respect to the main speed.
2. Adjustment range of open structure.
3. Stable regulation.
4. Permissible load— $T = T_n$ when downregulating with respect to the main speed, and $P = PH$ when adjusting upregulating.
5. This method requires the use of a frequency converter (FC)—a device that controls the frequency and amplitude of the output voltage.

In most cases, the regulation of the rotor speed of the IM with a phase rotor is carried out by introducing additional resistance R into the rotor winding circuit.

Figure 3b shows the natural (1) and artificial (2 and 3) mechanical characteristics of the IM for various values of additional resistance in the rotor winding circuit. At a given moment of resistance on motor shaft M_C equal to rated torque T_n , the nominal rotor speed

for each of the mechanical characteristics is different, since it is determined by points 1, 2, and 3 of the intersection of the straight line $M_c = M_n$ and by mechanical characteristics 1, 2, and 3. The slip ratio at T_n is $s_3 > s_2 > s_1$.

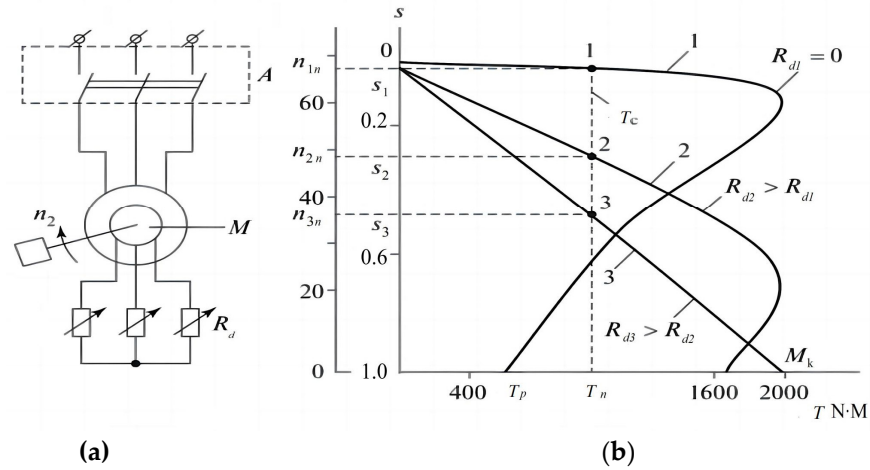


Figure 3. Regulation of the speed of rotation: (a) switching circuit; (b) mechanical characteristics. (b) The vertical axis represents speed and slip. The horizontal axis represents torque.

The disadvantages of the considered motor-speed-control method are significant energy losses in the control resistor; low rigidity of the mechanical characteristics, so that a small change in torque on the shaft causes a significant change in rotation speed; and discrete regulation of rotation speed. The considered method is used in systems where the operation based on artificial mechanical characteristics is short (for example, in starting and braking modes), and the main operation time of the motor is under the natural mechanical characteristic.

The electromechanical driving function diagram of the 11200 belt conveyor for ore transportation is shown in Figure 4. Induction motor M is controlled by an intermediate frequency converter. The power part of the converter consists of a rectifier (B), an LC filter (Φ), and an off-line voltage inverter. Single-chip microcomputer MK controls the keys of the inverter by realizing PWM pulse width modulation. The system is automatically controlled by a PLC programmable controller, which inputs speed change signals and safety fence sensor signals.

3.2. Method of Motor Selection

The mechanical part of the electric drive of the MKL1-1200 conveyor for transporting ore consists of an electric motor, a gearbox, and a drive drum. The kinematic diagram of the MKL1-1200 conveyor is shown in Figure 5.

Mechanism parameters:

Nominal belt speed: $V_{HOM} = 3.10$ m/s

Drive drum diameter: $D_b = 1.2$ M

Rotation angular velocity of drive drum:

$$\omega_b = \frac{2 * V}{D_b} = \frac{2 * 3.10}{1.2} = 5.17 \text{ rad/s} \tag{4}$$

In order to analyze the motion of the mechanical part of the electric drive, the actual kinematic diagram is transferred to the calculation diagram, in which the mass, moment of inertia, and stiffness of moving elements, as well as the forces and moments acting on these elements, are converted into the equivalent of the same speed-motor shaft.

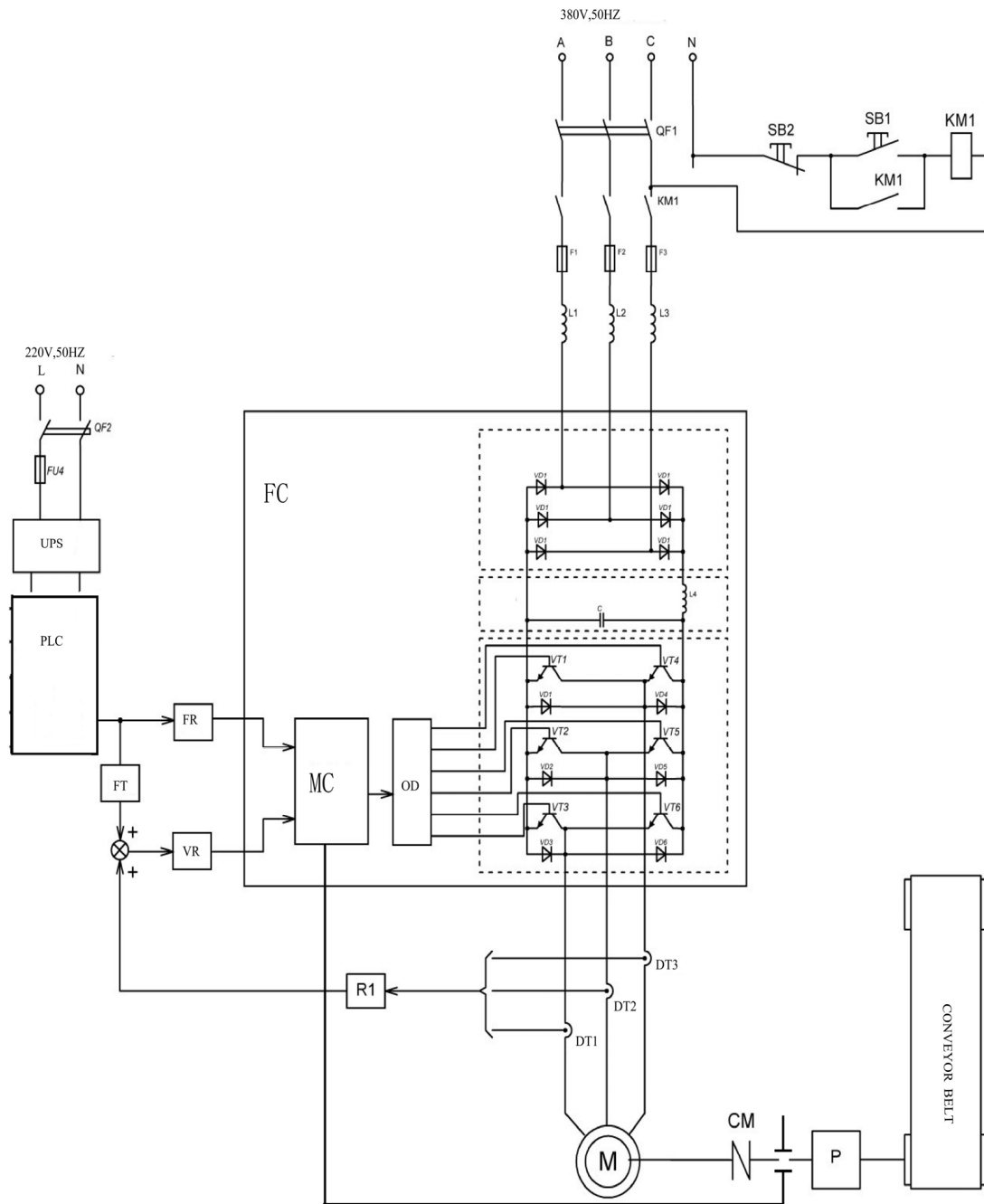


Figure 4. Functional diagram of the MKL1-1200belt conveyor: FC—frequency converter; MC—microcontroller; PLC—Programmable Logic Controller; R1—feedback resistor; FT—function transformer; PO—working mechanism (conveyor belt); VR—voltage regulator; FR—frequency regulator; OD—output device.

The process of switching to calculation diagrams is usually referred to as a reduction, and the values themselves are reduced. It is usually convenient and practical to carry out a reduction to motor speed. In these cases, the multi-mass mechanical part of the drive is replaced by one equivalent mass with moment of inertia J , which is influenced by electromagnetic torque of the motor M and the total reduced to motor shaft load torque M_c . Load torque M_c includes all external forces applied to the mechanical system, except for motor torque M .

The calculation diagram of the drive mechanical parts of the conveyor is shown in Figure 6.

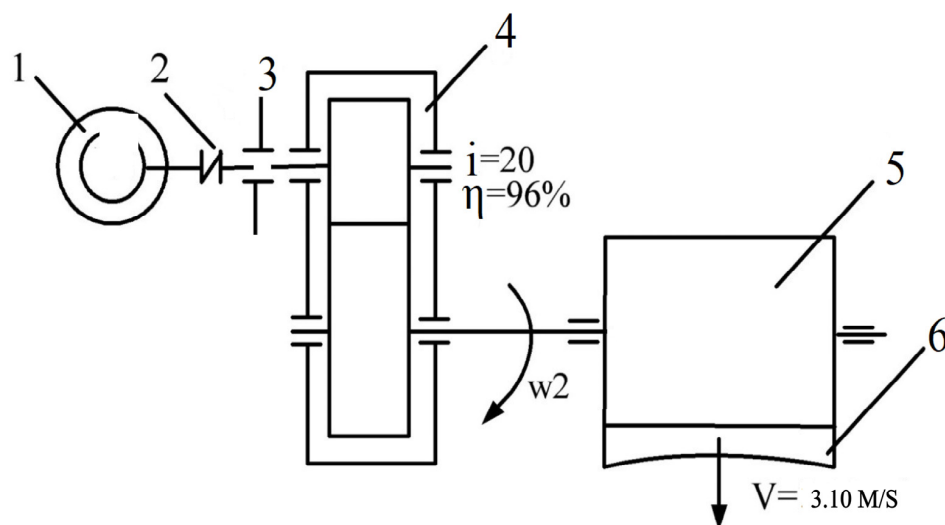


Figure 5. Kinematic diagram of the MKL1-1200conveyor: 1—motor; 2—motor; 3—brake; 4—cylinder reducer; 5—drive drum; 6—conveyor belt; ω_2 —angular velocity of drive drum.

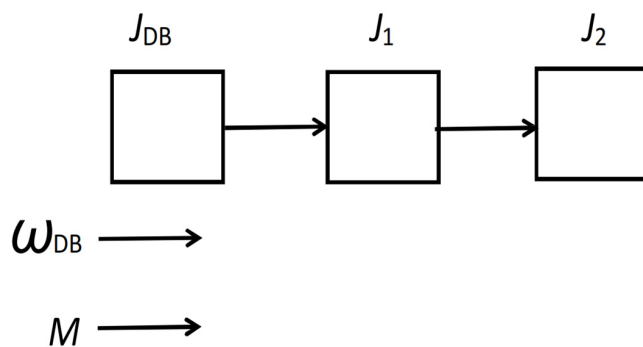


Figure 6. Calculation diagram of electric drive mechanical part: J_{DB} —engine moment of inertia; J_1 —moment of inertia of coupling; J_2 —moment of inertia of reducer; ω_{DB} —engine angular velocity; M —electromagnetic torque of engine.

According to the obtained data, the mechanical characteristic curve is drawn in Figure 7.

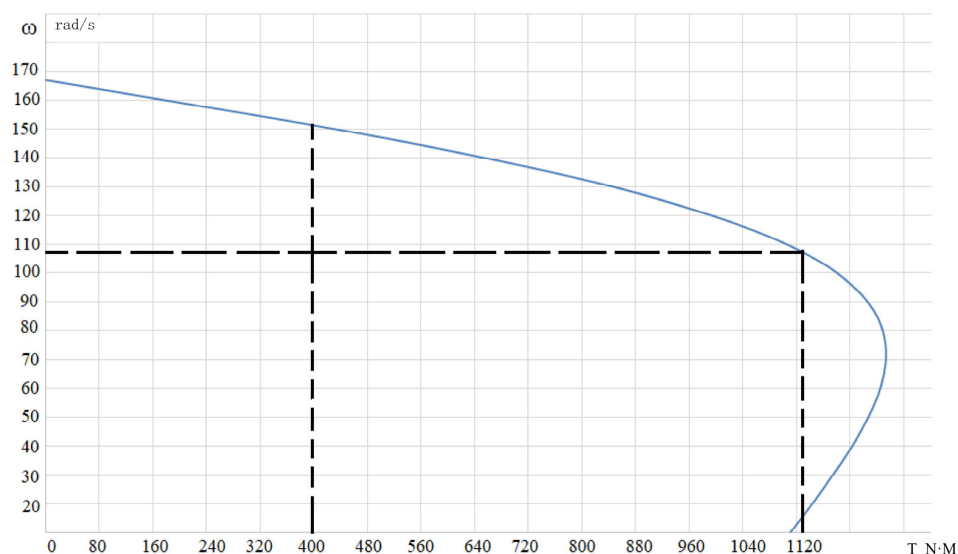


Figure 7. Mechanical Characteristic Curve ($M_{mex} = f(\omega)$).

The typical working cycle of a conveyor drive includes accelerating to the rated speed, moving at a constant speed of 3.10 m/s, and braking. After the conveyor starts, its running time is 12 h, which is 43,200 s, followed by an interruption of 10,800 s. The working cycle is 15 h long. Based on the calculation results, we constructed a mechanism load and speed graph (Figure 8).

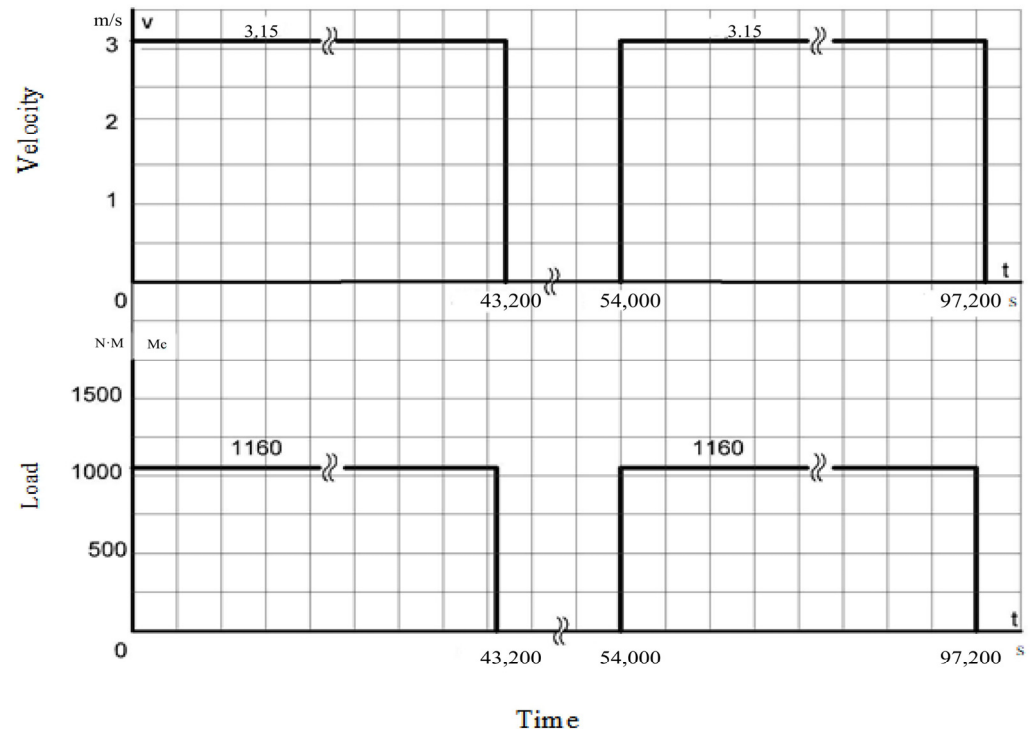


Figure 8. Load and velocity diagrams of mechanism.

Since the conveyor operates in continuous mode with alternating load, the dynamic processes (starting and braking modes) have practically no effect on the electric motor temperature. Therefore, the electric motor is selected on the basis of the static capacity of the machine.

The motor is selected according to the installation mode and environmental protection mode of the motor. With the calculations of preliminary power according to the catalogue, we can select an asynchronous motor.

Thus, the motor selected using this method meets the necessary conditions of heating, overload capacity, and starting properties.

3.3. Designing an Electrical Energy Converter

It is reasonable to choose a frequency converter as the regulating device. When the frequency converter is operational, the frequency of the controlled engine starts to accelerate smoothly without increasing the starting current and mechanical impact, thus reducing the burden on the engine and related transmission mechanisms and prolonging its service life. Frequency modulation can solve a major disadvantage of squirrel-cage motors, and the rotor speed of the motor is constant and has nothing to do with load. Frequency control can control the speed of the motor according to the nature of the load. This, in turn, avoids complex transient processes in the power grid and ensures that the equipment operates in the most economical mode.

Frequency control can also improve the trouble-free operation and durability of the process system. This is achieved by reducing the starting current, eliminating system component overload, and gradually generating equipment motorcycle hours. The frequency converter, different from other motor-speed-regulating devices, such as hydraulic coupling and mechanical transmission, can avoid various defects in system operation. We are talking

about the narrow adjustment range of equipment, difficult operation, poor quality of work, and uneconomical system as a whole.

Inverters combine unique quality, high technical level, reliability, and low price. On the basis of a frequency converter, flexible electric drive systems and process parameter adjustment systems can be created.

Inverters provide comprehensive electronic protection of the inverter and motor against overcurrent, overheating, ground leakage, and transmission line breakage. Converters allow tracking and displaying the main parameters of the system—given speed, output frequency, motor current and voltage, output power and torque, discrete input state, total running time of the converter, etc., on a digital console.

Converters by Siemens, ABB, Omron, Mitsubishi, and other companies are very common. Siemens converters focus on applications in the field of turbine mechanisms; Omron converters are inferior to ABB and Mitsubishi in their product line. Comparing the latter two manufacturers, the price of an ABB converter is higher. Further, Mitsubishi's guidance on a wide range of tasks is also beneficial. They are used in many fields, from turbomachinery to machinery manufacturing. Mitsubishi is famous for producing reliable and perfect equipment. Therefore, we were guided by these facts when choosing a converter.

For the selection of inverter size electrical energy, in accordance with the calculation of variables, we selected Siemens 6SE7132-1HF61-5BA0. For the corresponding inverter standard size, we selected power circuit equipment according to the catalogue. The output filter DU/DT was designed to reduce voltage rise, engine heating, and engine insulation from load and noise. We selected the 6SL3000-2AH32-4AA0 filter type. A contactor is a two-position electromagnetic device designed to frequently switch power circuits on and off remotely. The power circuits were in normal operation. We selected a 3RT1456 mains-type contactor with nominal current. A contactor is a two-position electromagnetic device designed to frequently switch power circuits on and off remotely. The power circuits were in normal operation. In order to simplify a set of motor power circuits, the power converter and the terminal located on the front panel of the module were connected to the corresponding motor image memory circuit, and a power module was used. We selected Model G 130 Power Module 6SL331016A32-2AA3. Its parameters are shown in Table 2.

Table 2. The parameters of the components.

| Type | Parameter | Value |
|--------------|-----------------------|---|
| Inverter | Power | Three-phase $3 \times 660/690$ V supply voltage |
| | Rated motor power | 200 kW |
| | Rated output current | 208 A |
| | Output frequency | 0–400 Hz |
| | Acceleration time | 0–3600 s |
| | Weight | 1200 kg |
| Filter | Rated current | 215 A |
| | Power loss | 0.425 kW |
| | Inductance | 150 μ Hn |
| | Voltage | 3 ph 660–690 V |
| | Nominal current | 270 A |
| | Output frequency | 50–60 Hz |
| Contactor | Nominal current | 250 A |
| | Number of power poles | 3P |
| | Control coil voltage | 127 V |
| Power module | Rated power | 200 kW |
| | Rated current | 215 A |
| | Supply voltage | 660–690 V |

4. Experimental Verification and Design of Algorithm

4.1. Design of Mathematical Models (Equations and Structural Circuits)

Recently, a new method for constructing frequency converter asynchronous motor systems was developed based on the fully differential energy levels recorded according to generalized motor theory. This method makes it possible to construct a frequency control system structure, called drive control system, and analyze and synthesize asynchronous electric drives in a simpler way. For this purpose, the modified electric drive coordinates in a fixed coordinate system are converted into a rotating coordinate system, where the electric drive coordinates are treated as vectors. From these values placed in projection form on the rotating coordinate axis, coordinate transformations are used to separate values proportional or constant with respect to the electric drive coordinates, which are used as control signals in the EP system. The differential equations of generalized machines are recorded in different coordinate systems. The α - and β -coordinate axes are not movable relative to the stator, and the D- and Q-axes are not movable relative to the rotor. Recording equations on these axes is a special case of the atheist description of machine processes. In general, the equation is written relative to any coordinate axes, such as U and V, rotating at the speed of ω_k , from which any special case of motor operation can be obtained. If the U-axis is real and the V-axis is imaginary, then the differential equation can be written in vector form.

$$\left. \begin{aligned} \overline{U}_1 &= R_1 \overline{i}_1 + \frac{d\overline{\psi}_1}{dt} + i \cdot W_k \cdot \overline{\psi}_1 \\ \overline{U}_2 &= R_2 \overline{i}_2 + \frac{d\overline{\psi}_2}{dt} + i \cdot (W_k - W) \cdot \overline{\psi}_2 \\ M &= \frac{m}{2} p_n L_{12} I_m (\overline{i}_1 \cdot \overline{i}_2) \\ \overline{\psi}_2 &= L_2 \overline{i}_2 + L_{12} \end{aligned} \right\} \quad (5a)$$

where $U_1, U_2, i_1, i_2, \psi_1, \psi_2$ —voltage, current, and flux chains of the stator (index 1) and rotor (index 2) coils; R_1, R_2 , and L_2 —active resistance and phase inductance of stator and rotor windings; L_{12} —mutual inductance between stator winding and rotor winding, and vice versa; W —electrical speed of the rotor; M —electromagnetic torque of the machine; i_2 —complex conjugate value; m —number of winding phases; p_n —number of machine poles; and I_m —imaginary part of a complex variable.

$$\left. \begin{aligned} U_{1U} &= R_1 \cdot i_{1U} + \frac{d\psi_{1U}}{dt} - W_k \psi_{1V} \\ U_{1V} &= R_1 \cdot i_{1V} + \frac{d\psi_{1V}}{dt} - W_k \psi_{1U} \\ U_{2U} &= R_2 \cdot i_{2U} + \frac{d\psi_{2U}}{dt} - (W_k - W) \psi_{2V} \\ U_{2V} &= R_2 \cdot i_{2V} + \frac{d\psi_{2V}}{dt} - (W_k - W) \psi_{2U} \end{aligned} \right\} \quad (5b)$$

where $\psi_{1U}, \psi_{1V}, \psi_{2U}, \psi_{2V}$ —projections of stator and rotor vectors on the U- and V-axes.

According to the state variables used by the machine, the electromagnetic moment equation of the machine can have different forms. Especially when selecting the current and chain of the stator and rotor as the basic variables, the torque is recorded in the following three forms:

$$\left. \begin{aligned} M &= \frac{m}{2} p_n \cdot (\psi_{1U} \cdot i_{1V} - \psi_{1V} \cdot i_{1U}); \\ M &= \frac{m}{2} p_n \cdot (\psi_{2V} \cdot i_{2U} - \psi_{2U} \cdot i_{2V}); \\ M &= \frac{m}{2} \left(\frac{p_n L_{12}}{L_1 L_2 - L_{12}} \right) \cdot ((\psi_{1V} \cdot i_{2U} - \psi_{1U} \cdot i_{2V})) \end{aligned} \right\} \quad (5c)$$

Expressions (5a)–(5c) provide the possibility of recording equations on any axis. We now describe the electromechanical processes that occur in communication machines. There are three main types of speeds on the coordinate axis: $W_k = 0$; $W_k = W$; $W_k = W_0$.

In order to describe the process of frequency vector control in asynchronous motors, it is best to choose $W_k = W_0$, which greatly simplifies the calculation. The coordinate systems X and Y can rotate at different speeds, depending on the vector of the coordinate

system. In setting mode, speed W_0 is the synchronous speed of AD ($W_0 = 2\pi f_1$). By changing the position of the coordinate system to correctly select vectors, the synthesis of the differential equation and control system of the electric motor can be simplified. The transition from a generalized machine to a true three-phase asynchronous machine is achieved using coordinate transformation equations and replacing the parameters of the generalized machine with real parameter phase values.

The coordinate transformation of a generalized equation is called straight-line equation, and vice versa. The coordinate transformation formula is derived when the power of two machines remains constant. They are used to record any variable on any axis. For example, the direct conversion formulas for stator currents (I_{1A} , I_{1B} , and I_{1C}) on the α - and β -axes of generalized machines A , B , and C are as follows:

$$\begin{aligned} i_{1\alpha} &= \frac{2}{3}K_C \cdot i_{1A} \\ i_{\beta} &= \frac{\sqrt{3}}{2}K_C(i_{1B} - i_{1C}) \end{aligned} \quad (5d)$$

Reverse conversion formula:

$$\begin{aligned} i_{1A} &= K_C \cdot i_{1\alpha}; \\ i_{1B} &= K_C \cdot \left(-\frac{1}{2} \cdot i_{1\alpha} + \frac{\sqrt{3}}{2} \cdot i_{1\beta}\right); \\ i_{1C} &= K_C \cdot \left(-\frac{1}{2} \cdot i_{1\alpha} - \frac{\sqrt{3}}{2} \cdot i_{1\beta}\right) \end{aligned} \quad (5e)$$

where $K_C = 2/3$ —matching coefficient.

In order to achieve vector control of short-circuit asynchronous motors, the x -axis should be oriented in the direction of resulting rotor Ψ_2 . In this case, the coordinate systems x and y rotate in space at the speed of the rotor field, which is W_0 . Therefore, we have the following relationship:

$$\begin{aligned} \psi_{2X} &= \psi_2; \\ \psi_{2Y} &= 0 \end{aligned} \quad (5f)$$

The form of the differential equation is

$$\left. \begin{aligned} U_{1X} &= R_1 \cdot i_{1X} + \frac{L_{12}}{L_2} \cdot \frac{d\psi_2}{dt} + \left(L_1 - \frac{L_{12}^2}{L_2}\right) \cdot \left(\frac{di_{1X}}{dt} - i_{1X} \cdot W_0\right); \\ U_{1Y} &= R_1 \cdot i_{1Y} + \frac{L_{12}}{L_2} \cdot \psi_2 \cdot W_0 + \left(L_1 - \frac{L_{12}^2}{L_2}\right) \cdot \left(\frac{di_{1Y}}{dt} - i_{1Y} \cdot W_0\right); \\ 0 &= \frac{R_2}{L_2} \psi_2 + \frac{d\psi_2}{dt} - R_2 \frac{L_{12}}{L_2} i_{1X}; \\ 0 &= R_2 \frac{L_{12}}{L_2} i_{1X} - \psi_2 W_2; \\ M &= \frac{3}{2} p_n \frac{L_{12}}{L_2} \psi_2 i_{1Y}; \end{aligned} \right\} \quad (5g)$$

where U_{1X} , U_{1Y} , I_{1X} , and I_{1Y} —projection of motor stator voltage and current vectors on the X - and Y -axes; 2 —result modulus of the rotor flux coupling vector; and W , W_0 , and W_2 —circular slip frequency of the rotor relative to the rotor field.

The resulting AD structure is a complex interconnected control chain system. However, it makes it possible to more easily study the dynamic characteristics of the engine under given and disturbance effects and determine engine parameters using modeling methods. The structural diagram can be greatly simplified by compensating for the effects in the system, which are defined by the internal coupling of the motor when using decoupling blocks.

4.2. Selection

It is feasible to study the static and dynamic performance of a computer-aided electric drive system, and it can be simulated using a computer according to its mathematical model. The current situation of computer technology and related software makes it possible to simulate various objects in the fastest, most convenient, and most flexible way and obtain

reliable results. A computer model avoids physical simulation, that is, the real embodiment of the system under study, and provides convenience for changing model parameters.

Matlab software was selected to realize the mathematical model. The Matlab interactive system includes a visual simulation tool, simulink, which was used to simulate the mathematical model of the computer-aided electric actuator. Continuous components were used as units for system modeling, because the frequency of modern controllers is high enough to receive discrete signals as continuous signals. Since all the necessary calculations were performed in the previous section, we set up all the blocks of the simulation model. Some elements were implemented as subsystems using the “subsystem” unit. Each subsystem has its own name. It is necessary to give the structure diagram of these units.

The model adopts subsystems of “frequency converter”, “phase converter”, “coordinator”, “flow channel”, “speed channel”, and “flow and rotation detection”.

The structure diagram of the subsystem model of “frequency converter” is shown in Figure 9.

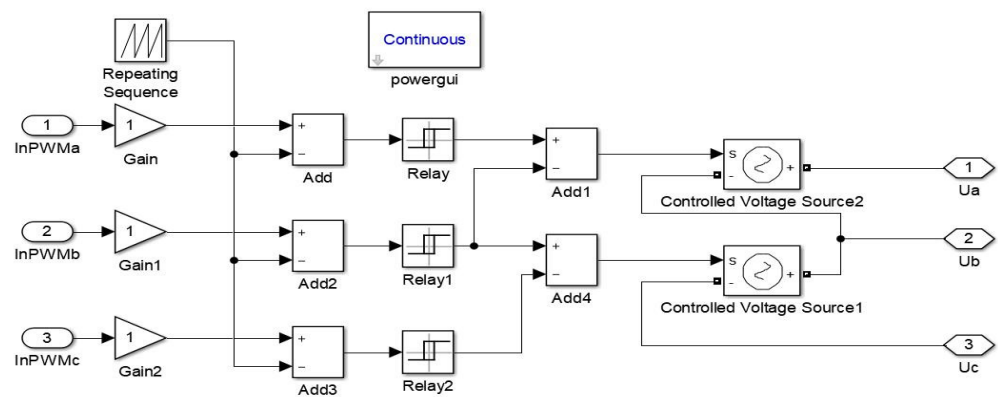


Figure 9. Structure diagram of subsystem model “frequency converter”.

Figures 10 and 11 show the model structure diagrams of the “phase converter” subsystems of voltage and current.

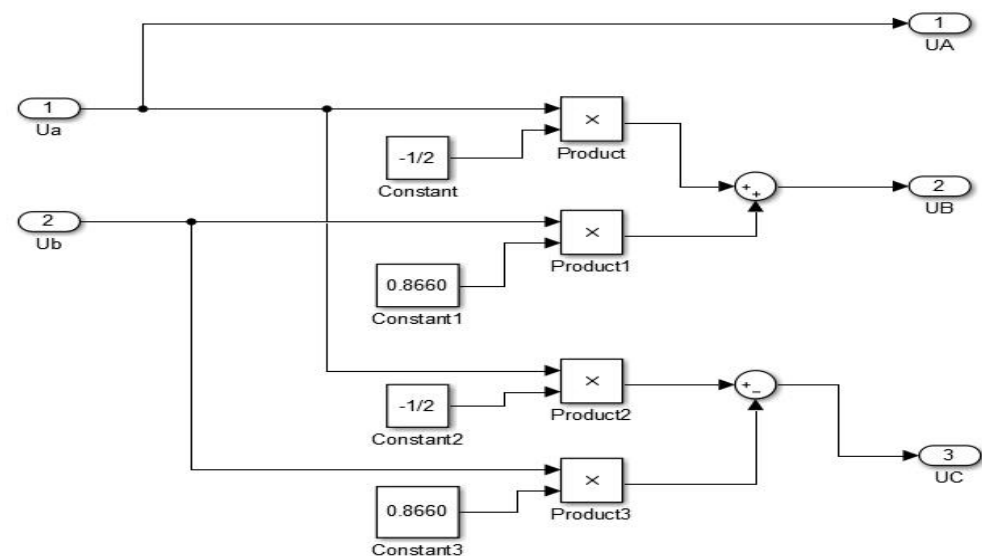


Figure 10. Block diagram of the “phase converter” subsystem model of voltage.

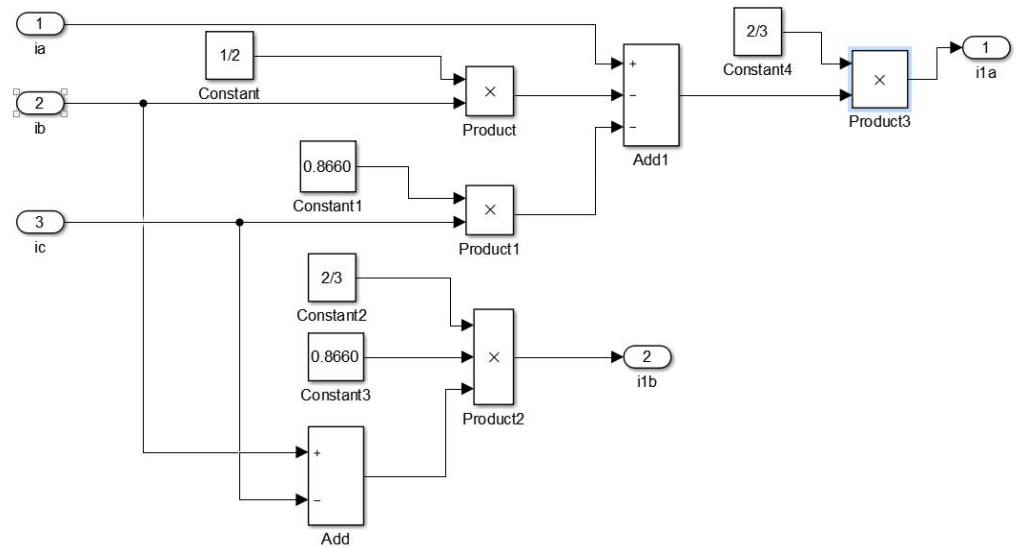


Figure 11. Block diagram of the subsystem model “Phase converter” of current.

Model structure diagrams of the coordinate converter subsystem for voltage and current are shown in Figures 12 and 13.

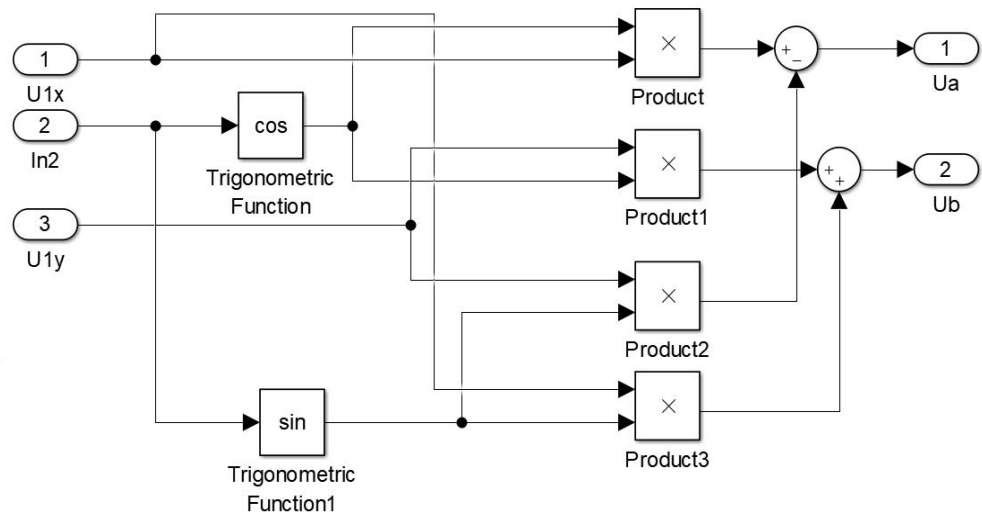


Figure 12. Structure diagram of subsystem model “coordinate converter” of voltage.

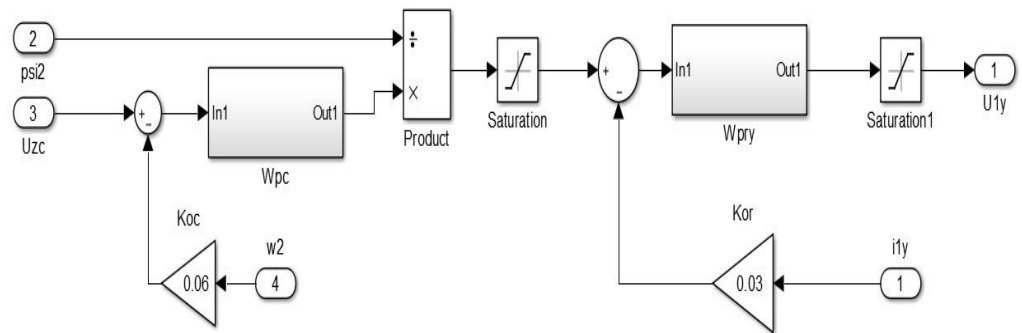


Figure 13. Structure diagram of speed channel subsystem model.

The structure diagram of the flow channel subsystem model is shown in Figure 13.

4.2.1. Calculation of Periodic Transient State of Mechanism and Determination of Quality Index

Figures 14 and 15 show the graphs obtained in the figure results of simulation modeling in the Matlab environment.

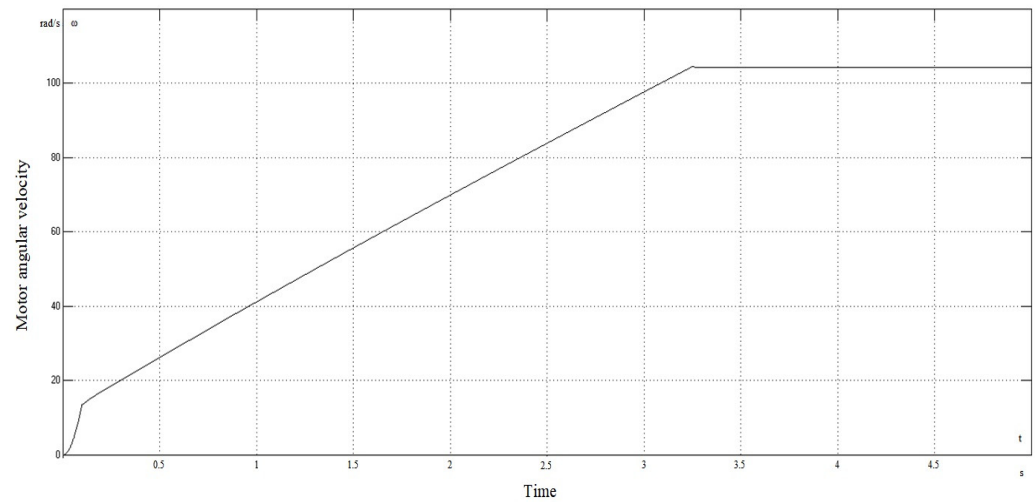


Figure 14. Angular velocity change diagram.

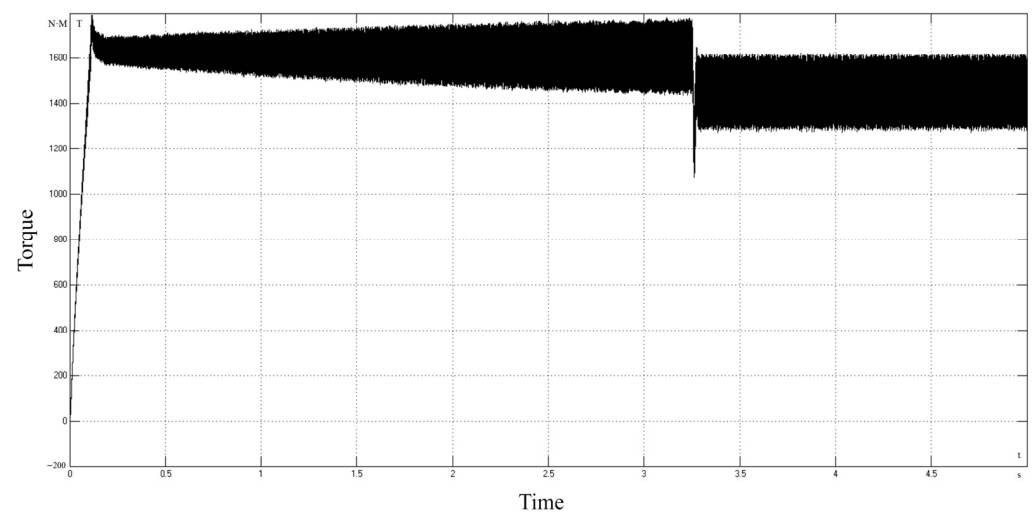


Figure 15. Engine Torque Variation Diagram.

The angular velocity rapidly increased from 0 to 0.1 s and then uniformly increased from 0.1 to 3.2 s. After reaching the maximum value at 3.2 s, it slightly decreased and maintained stability.

The engine torque rapidly increased from 0 to 0.1 s and then uniformly increased from 0.1 to 3.2 s. After reaching the maximum value at 3.2 s, it slightly decreased and maintained stability.

4.2.2. Comparative Analysis of the Obtained Quality Index and the Electric Drive Requirements of the Mechanism

According to the transient curve obtained from the simulation of the mechanism electric drive system, the obtained quality index can be compared with the requirements of the mechanism electric drive. The transition timetable shows the following:

- (1) The acceleration speed in the starting process was roughly constant without setbacks, which meets the transient quality requirements;

- (2) The smooth start of the engine was ensured, and the torque and acceleration values were limited at the same time;
- (3) The speed accuracy was kept within the allowable value.

4.2.3. Checking the Heating Capacity of the Motor and the Overload Capacity of the Electric Drive According to the Accurate Load Diagram of the Mechanical Device per Working Cycle

Because the engine is operated in variable load mode for a long time, there is no need to check it for heating. When the engine runs under this working condition, the temperature cannot reach the maximum allowable temperature.

4.3. Design of Control Program Algorithm

Based on the conveyor operation described in the previous paper, a control program algorithm can be constructed. The algorithm of the control program is shown in Figure 16.

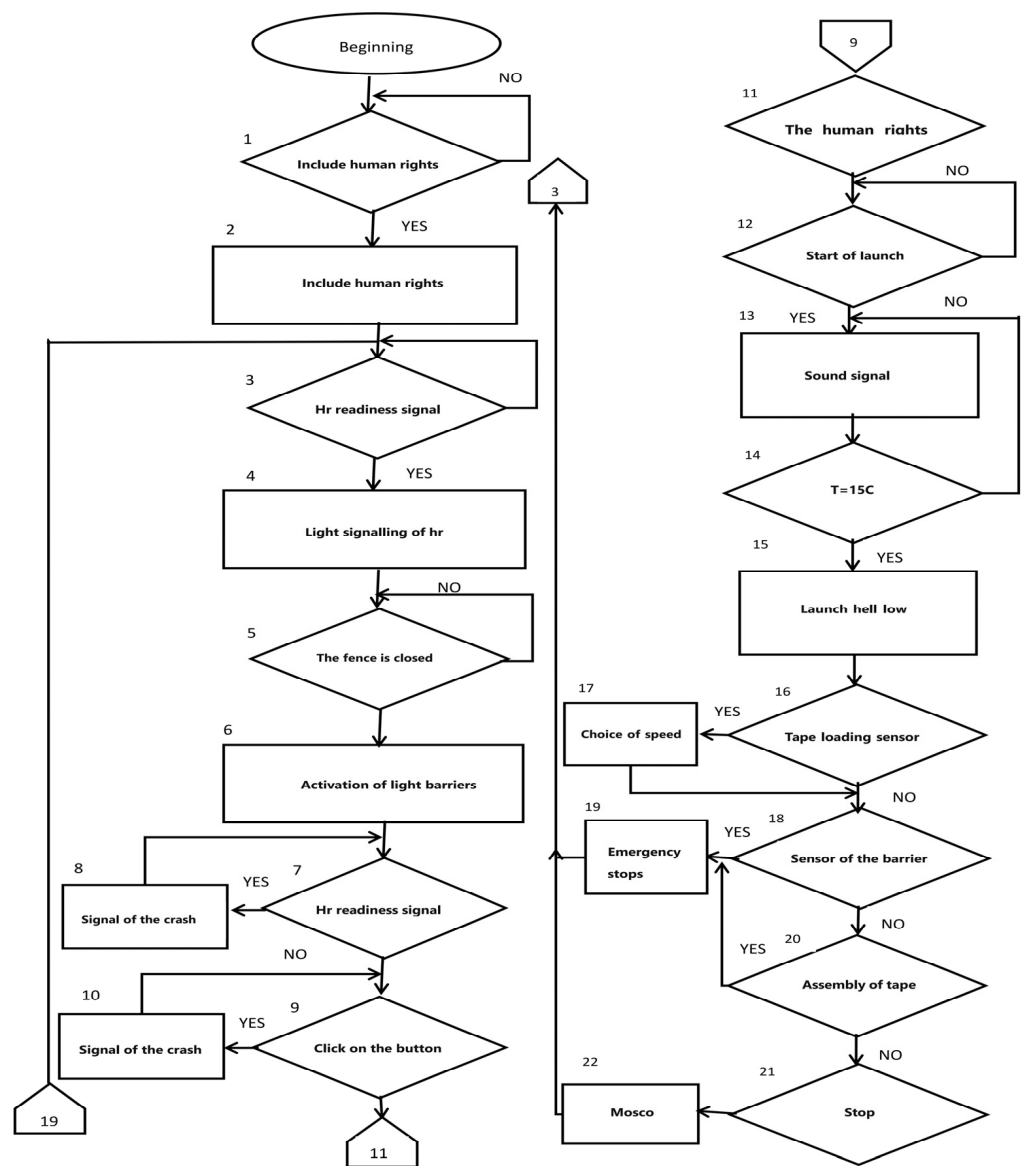


Figure 16. Block diagram of basic program algorithm.

5. Conclusions

In accordance with the task of research qualification work, the calculation of the automated electric drive of the MKL1-1200 main conveyor for ore movement was carried out. As a result, this work developed calculations, explanatory notes, and graphic applications.

During this work, an analysis of the technological process of the conveyor, as well as a detailed analysis of the electric drive, was carried out. For the installation of the electric drive system created, the test motor VAO2-315M6 and the frequency converter Siemens model 6SE7132-1HF61-5BAO ($P_n = 160$ kW) were chosen. An automatic control system was designed based on the controller Siemens S7-1200; then, a mathematical model of an automated electric drive was developed. Based on the mathematical model, a simulation model of the automatic electric drive was built, and the modes were modeled. After designing, the obtained plots of transients completely corresponded to the required transients, which means that the automatic control system (ACS) parameters were calculated quite accurately and the conveyor electric drive met all requirements.

Under industrial conditions, there is a high possibility of using the design scheme proposed in this article, which can narrow the debugging range of experimental parameters for specific implementation processes.

Author Contributions: The presented work was under the supervision of Y.L. and L.W. in terms of conceptualization, methodology, software, and writing—original draft; H.L. in terms of validation and writing—review and editing; J.H. and J.Z. in terms of methodology and writing—review; L.T. and W.W. in terms of validation. All authors have read and agreed to the published version of the manuscript.

Funding: This research was funded by National Natural Science Foundation of China (No. 52005188) and The Agricultural Science and Technology Cooperation and Construction Project of the New Rural Development Research Institute of South China Agricultural University—Demonstration and Promotion of Mechanization Technology for Transporting Fruit and Tea Plantations in Hilly and Mountainous Areas ((No. 2021XNYNYKJHZGJ039).

Institutional Review Board Statement: Not applicable.

Informed Consent Statement: Not applicable.

Data Availability Statement: This study does not report any data.

Acknowledgments: The authors acknowledge the editors and reviewers for their constructive comments and all the support for this work.

Conflicts of Interest: The authors declare no conflict of interest.

References

1. Yang, C.; Bu, L.; Chen, B. Energy modeling and online parameter identification for permanent magnet synchronous motor driven belt conveyors. *Measurement* **2021**, *178*, 109342. [[CrossRef](#)]
2. Niu, F.; Wang, B.; Babel, A.S.; Li, K.; Strangas, E.G. Comparative evaluation of direct torque control strategies for permanent magnet synchronous machines. *IEEE Trans. Power Electron.* **2015**, *31*, 1408–1424. [[CrossRef](#)]
3. Salvador, C.; Mascaró, M.; Ruiz del Solar, J. *Automation of Unit and Auxiliary Operations in Block/Panel Caving: Challenges and Opportunities*; Massmin: Santiago, Chile, 2020.
4. Fernando, H.; Marshall, J.A.; Larsson, J. Iterative learning-based admittance control for autonomous excavation. *J. Intell. Robot. Syst.* **2019**, *96*, 493–500. [[CrossRef](#)]
5. Alahmad, M.A.; Wheeler, P.G.; Schwer, A.; Eiden, J.; Brumbaugh, A. A comparative study of three feedback devices for residential real-time energy monitoring. *IEEE Trans. Ind. Electron.* **2011**, *59*, 2002–2013. [[CrossRef](#)]
6. Gao, L.; Fletcher, J.E.; Zheng, L. Low-speed control improvements for a two-level five-phase inverter-fed induction machine using classic direct torque control. *IEEE Trans. Ind. Electron.* **2010**, *58*, 2744–2754. [[CrossRef](#)]
7. Alharbi, F.; Luo, S.; Zhang, H.; Shaukat, K.; Yang, G.; Wheeler, C.A.; Chen, Z. A brief review of acoustic and vibration signal-based fault detection for belt conveyor idlers using machine learning models. *Sensors* **2023**, *23*, 1902. [[CrossRef](#)] [[PubMed](#)]
8. Suetake, M.; da Silva, I.N.; Goedel, A. Embedded DSP-based compact fuzzy system and its application for induction-motor V/f speed control. *IEEE Trans. Ind. Electron.* **2010**, *58*, 750–760. [[CrossRef](#)]

9. Jeftenić, B.; Ristić, L.; Bebić, M.; Štatkić, S. Controlled induction motor drives supplied by frequency converters on belt conveyors—Modeling and commissioning. In Proceedings of the 2009 35th Annual Conference of IEEE Industrial Electronics, Porto, Portugal, 3–5 November 2009; pp. 1063–1068.
10. Middelberg, A.; Zhang, J.; Xia, X. An optimal control model for load shifting—with application in the energy management of a colliery. *Appl. Energy* **2009**, *86*, 1266–1273. [[CrossRef](#)]
11. Kulinowski, P.; Kasza, P.; Zarzycki, J. Influence of design parameters of idler bearing units on the energy consumption of a belt conveyor. *Sustainability* **2021**, *13*, 437. [[CrossRef](#)]
12. Kusumaningtyas, I.; Lodewijks, G. Toward intelligent power consumption optimization in long high-speed passenger conveyors. In Proceedings of the 2007 IEEE Intelligent Transportation Systems Conference, Bellevue, WA, USA, 30 September–3 October 2007; pp. 597–602.
13. Zhang, S.; Xia, X. A new energy calculation model of belt conveyor. In Proceedings of the AFRICON, Nairobi, Kenya, 23–25 September 2009; pp. 1–6.
14. Zimroz, R.; Hardygóra, M.; Blazej, R. Maintenance of belt conveyor systems in Poland—An overview. In Proceedings of the 12th International Symposium Continuous Surface Mining-Aachen 2014; Springer: Cham, Switzerland, 2015; pp. 21–30.
15. Stefaniak, P.K.; Wyłomańska, A.; Obuchowski, J.; Zimroz, R. Procedures for decision thresholds finding in maintenance management of belt conveyor system—statistical modeling of diagnostic data. In *Proceedings of the 12th International Symposium Continuous Surface Mining-Aachen 2014*; Springer: Cham, Switzerland, 2015; pp. 391–402.
16. Szrek, J.; Wodecki, J.; Błażej, R.; Zimroz, R. An inspection robot for belt conveyor maintenance in underground mine—Infrared thermography for overheated idlers detection. *Appl. Sci.* **2020**, *10*, 4984. [[CrossRef](#)]
17. Zhao, M.H. Design of Patrol Robot System for Mining Belt Conveyor. In Proceedings of the 2018 10th International Conference on Intelligent Human-Machine Systems and Cybernetics (IHMSC), Hangzhou, China, 25–26 August 2018; Volume 2, pp. 1–3.
18. Käslin, R.; Kolvenbach, H.; Paez, L.; Lika, K.; Hutter, M. Towards a passive adaptive planar foot with ground orientation and contact force sensing for legged robots. In Proceedings of the 2018 IEEE/RSJ International Conference on Intelligent Robots and Systems (IROS), Madrid, Spain, 1–5 October 2018; pp. 2707–2714.
19. Soofastaei, A.; Karimpour, E.; Knights, P.; Kizil, M. Energy-efficient loading and hauling operations. In *Energy Efficiency in the Minerals Industry: Best Practices and Research Directions*; Springer: Cham, Switzerland, 2018; pp. 121–146.
20. Zhang, S.; Xia, X. Modeling and energy efficiency optimization of belt conveyors. *Appl. Energy* **2011**, *88*, 3061–3071. [[CrossRef](#)]
21. Gładysiewicz, L.; Konieczna-Fuławka, M. Influence of idler set load distribution on belt rolling resistance. *Arch. Min. Sci.* **2019**, *64*, 251–259.
22. Król, R.; Gładysiewicz, L.; Kaszuba, D.; Kisielewski, W. New quality standards of testing idlers for highly effective belt conveyors. In *IOP Conference Series: Earth and Environmental Science*; IOP Publishing: Bristol, UK, 2017; Volume 95, p. 042055.
23. Akparibo, A.R.; Normanyo, E. Application of resistance energy model to optimising electric power consumption of a belt conveyor system. *Int. J. Power Syst.* **2019**, *4*, 97–108. [[CrossRef](#)]
24. Youssef, G.S.; Taha, I.; Shihata, L.A.; Abdel-ghany, W.E.; Ebeid, S.J. Improved energy efficiency in troughed belt conveyors: Selected factors and effects. *Int. J. Eng. Tech. Res.* **2015**, *3*, 174–180.
25. Lutyński, A.; Kozubek, A. Eksploatacja przenośnika wznoszącego upadowej odstawczo-transportowej w KWK “Marcel”. *Maszyny Górnicze* **2010**, *28*, 13–18.
26. Szrek, J.; Jakubiak, J.; Zimroz, R. A mobile robot-based system for automatic inspection of belt conveyors in mining industry. *Energies* **2022**, *15*, 327. [[CrossRef](#)]

Disclaimer/Publisher’s Note: The statements, opinions and data contained in all publications are solely those of the individual author(s) and contributor(s) and not of MDPI and/or the editor(s). MDPI and/or the editor(s) disclaim responsibility for any injury to people or property resulting from any ideas, methods, instructions or products referred to in the content.